Macromolecules

ARTICLE

pubs.acs.org/Macromolecules

Anisotropic Hydrogel from Complexation-Driven Reorientation of Semirigid Polyanion at Ca^{2+} Diffusion Flux Front

Zi Liang Wu,[†] Takayuki Kurokawa,[‡,§] Daisuke Sawada,[†] Jian Hu,[†] Hidemitsu Furukawa,[‡,#] and Jian Ping Gong*[,‡]

[†]Division of Biological Sciences, Graduate School of Science, Hokkaido University, Sapporo 060-0810, Japan

[‡]Faculty of Advanced Life Science, Graduate School of Science, Hokkaido University, Sapporo 060-0810, Japan

[§]Creative Research Initiative Sousei, Hokkaido University, Sapporo 001-0021, Japan

Supporting Information

ABSTRACT: We report a macroscopically anisotropic hydrogel developed by the facile dialysis of a synthetic semirigid polyanion in aqueous solution of multivalent cations. By the uniaxial diffusion of Ca^{2+} into two ends of a thin rectangular reaction cell containing semirigid polyanion poly(2,2′-disulfonyl-4,4′-benzidine terephthalamide) (PBDT) aqueous solution, centimeter-scale anisotropic hydrogels with the PBDT molecules and their self-assembled fibrous bundles align in *perpendicular* to the Ca^{2+} diffusion direction are obtained. The anisotropic gel shows a higher elastic modulus and tensile fracture stress/strain in the direction parallel to the PBDT orientation than that of perpendicular direction. By observing *in situ* the gelation process, an extraordinary molecular reorientation of PBDT at the Ca^{2+} diffusion flux front is observed for the first time. The mechanism for the molecular reorientation is discussed in terms of complexation and gelation.

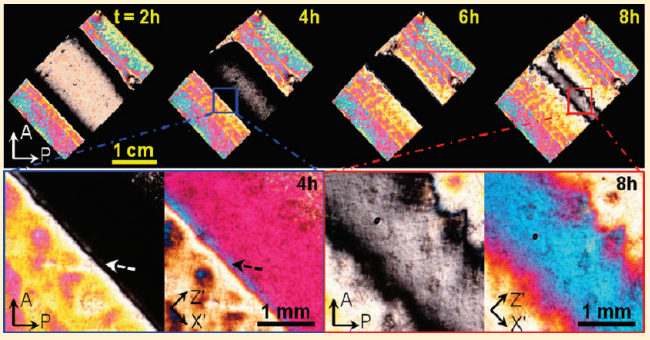

INTRODUCTION

Soft biotissues such as cartilage, muscle, and eyeball are in a wet gel-like state, including 30−80% water. These gels generally possess well-ordered structures that play a crucial role in executing the functions of living organisms.[1,2] For example, collagen fibers are closely packed with parallel arrays in tendons; these oriented collagen fibers endow the tendon with excellent mechanical properties.[1] Myosin shows a liquid-crystalline (LC) structure in sarcomere, contributing to the formation and smooth motion of muscle fibers.[1b,2b] In these biotissues, biomacromolecules such as DNA, filamentous actins (F-actin), and microtubules with rigid or semirigid structure and negative charges are significant to the formation of versatile self-assembled structures via noncovalent interaction.[3] It is well-known that a considerable amount of cationic proteins, liposomes, or multivalent cations are involved in the self-organization of these negatively charged semirigid biomacromolecules such as cytoskeleton organization and gene packaging.[4] These facts indicate the significance of electrostatic interaction during the self-assembly of biomacromolecules.

Inspired from the natural materials, lots of self-assembled structures of both biomacromolecules and synthetic polymers are developed in solutions and hydrogels by controlling the intermolecular ionic bonds, hydrophobic interactions and hydrogen bonds.[5] However, the oriented structures developed in the former works are usually limited in a submicrometer level, hydrogels with macroscopically anisotropic structure are rarely realized. Recently, we successfully developed hydrogels with millimeter-scale anisotropic domains by polymerizing a cationic monomer in the presence of a small amount of semirigid polyanion as dopant.[6] The semirigid polyion complex forms during the polymerization and self-assembles into ordered structures that are frozen by the subsequent chemically cross-linking process. Further increase in the size of anisotropic domains is difficult to achieve because of the occurrence of polyion condensation and resultant gel deformation.

A significant route to develop hydrogels with macroscopically anisotropic structure is through the reaction-diffusion process; the reaction and diffusion compete with each other and result in intricate spatial or temporal structures.[7] Dobashi and co-workers had developed a method to synthesize physical LC hydrogels in a semipermeable tube by dialyzing aqueous solutions of DNA or Curdlan in a multivalent cation solution, where biomacromolecules with semirigid structure and negative charges can form complexation with the multivalent cation.[8] The cationic ion diffusion into the dialysis tube induces the molecular orientation and physical gelation to form cylindrically symmetric structure up to the size of several centimeters. They claimed that the biomolecules orient along the cationic ions diffusion direction to form a radial structure.

Received: January 17, 2011
Revised: March 8, 2011
Published: March 23, 2011

In this paper, we report the synthesis of macroscopically anisotropic hydrogels by dialysis of a synthetic semirigid polyanion poly(2,2′-disulfonyl-4,4′-benzidine terephthalamide) (PBDT) into aqueous solution of multivalent cations Ca^{2+}. The orientation and gelation of PBDT molecules are induced and controlled by the diffusion process of Ca^{2+}. We demonstrate that PBDT molecules form mesoscopic fibrous bundles during the complexation process; PBDT and its bundle self-assemble at the diffusion front and align *perpendicular* to the Ca^{2+} diffusion direction, as confirmed by polarizing microscopy observation, small-angle X-ray scattering, and tensile test of the gel. This is different from that of DNA and Curdlan systems that were reported showing *parallel* orientation to the ion diffusion direction.

The hydrogels of synthetic PBDT with an ordered structure have some advantages over the biomacromolecules of DNA and Curdlan that have secondary structure, such as a wider window in thermal stability, pH, etc. The development of hydrogel with complex anisotropic structure and finding of molecular reorientation during the dialysis process should merit clarifying the hidden formation mechanism of macroscopically ordered structures in living organisms.

EXPERIMENTAL SECTION

Synthesis of Physical LC Hydrogel via Dialysis. PBDT, a water-soluble semirigid polyanion, was synthesized by an interfacial polycondensation reaction.[9] The synthesized PBDT has a super high weight-average molecular weight, $M_w \sim 2.1 \times 10^6$ g/mol. The aqueous solutions of PBDT were prepared by dissolving a prescribed amount of PBDT into pure water; the critical concentration of nematic liquid crystal, C_{LC}*, is 2 wt %. The physical LC gels can be synthesized via the diffusion of Ca^{2+} into solutions with different PBDT concentrations, C_P. Although the concentration of Ca^{2+} is another important factor to affect the dialysis process, we keep it constant here as 0.5 M for simplicity while the PBDT concentration, C_P, was changed from 1 to 3 wt %, covering the range below and above the C_{LC}*. The PBDT solution with different C_P was poured into a thin rectangular cell (dimensions: 30 mm ×20 mm ×1 mm), consisting of a pair of parallel glass plates separated by a silicone spacer with a 1 mm thickness (Figure 1a). Two opposite sides were wrapped by dialysis membranes (BX-100, Bel-Art Products, USA) to permit uniaxial diffusion of multivalent cations into the reaction cell. The cell containing the PBDT solution was dialyzed to 200 mL of 0.5 M calcium chloride ($CaCl_2$) solution at room temperature. The gelation front progressed from the two open rims of the cell to the interior within 10 h, and plate physical PBDT gel with slight turbidity was obtained after 1 day in order to reach the diffusion equilibrium.

Observation under Polarizing Optical Microscope (POM). LC structures of the synthesized gels were identified using POM (Nikon, LV100POL). A 530 nm tint plate was applied to distinguish the PBDT molecular orientation in the synthesized gel. The entire image of the entire LC gel was obtained by stacking dozens of local micrographs. The diffusion and gelation process were monitored by observing the sample at different dialysis time under POM. The birefringence, Δn, was measured from the retardation values using a Berek compensator. To study the effect of different ions in swelling solution on the self-assembled structure of LC gel, the as-prepared gels were swelled into pure water and solutions with different salts, 0.5 M $CaCl_2$ or 1.5 M NaCl, and then the birefringence was measured under POM at different swelling time.

Swelling Ratio of Gels. The swelling ratio, q, of the outer and central regions of swollen gel (i.e., region I and region II shown in Figure 1b, respectively) defined as the mass ratio of the sample in its swollen state to its dried state was estimated. The dried samples were obtained by keeping them in a desiccator for 12 h and in a vacuum oven at 60 °C for 6 h.

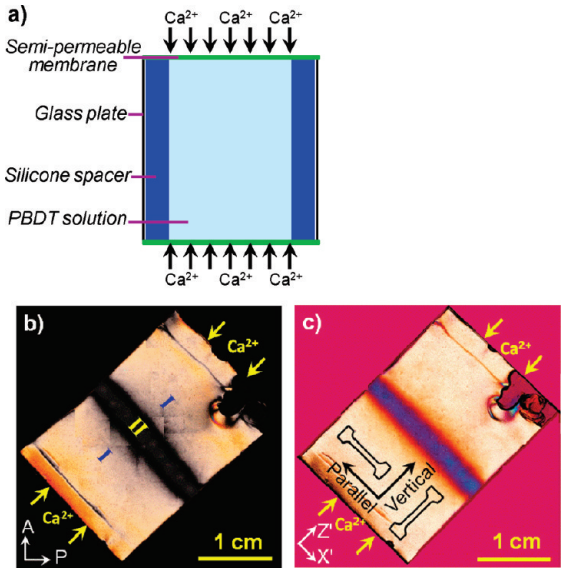

Figure 1. (a) Scheme of the reaction cell used for synthesizing physically cross-linked LC hydrogel by dialysis of PBDT solution in $CaCl_2$ solution; dimension of cell: 30 mm (length) × 20 mm (width) × 1 mm (thickness). (b, c) Images of synthesized 1 wt % gel observed under polarizing microscope; crossed polarizers (b), insertion of 530 nm tint plate (c). Arrows show the Ca^{2+} diffusion direction during the synthesis of the gel. The outer and central regions of the gel are denoted as region I and region II, respectively, as shown in part b; SAXS and tensile samples cut from the outer region of LC gel are shown in part c. Key: A, analyzer; P, polarizer; X′, fast axis of the tint plate; Z′, slow axis of the tint plate.

Tensile Tests of Physical LC Gels. The mechanical property of the gel was measured by tensile test using a commercial test machine (Tensilon RTC-1150A, Orientec Co.). The swollen gel in water was cut into a dumbbell shape standardized as the JIS-K6251−7 sizes (length: 35 mm; width: 6 mm; thickness: ∼1 mm; gauge length: 12 mm; inner width: 2 mm) with a gel cutting machine (Dumbbell Co., Ltd.). The stress−strain curve was recorded while the sample was stretched at a constant rate of 100 mm/min. Two kinds of samples were cut from the outer region of the gel (region I) in directions perpendicular and parallel to the Ca^{2+} diffusion direction (i.e., parallel and perpendicular to the PBDT alignment direction), noted as Parallel and Vertical, respectively (Figure 1c). The elastic modulus of the gel was calculated by measuring the initial slope of the stress−strain curve ($\varepsilon < 0.1$).

Small Angle X-ray Scattering (SAXS). The dumbbell shape specimen of Parallel, as shown in Figure 1c, was cut from the region I of the anisotropic gels synthesized with C_P of 1 and 3 wt %. The relative scattering position on the specimen is shown in Figure 2a. The sample was covered by two Kapton films for the SAXS measurements performed at the BL40B2 of SPring-8, Japan Synchrotron Radiation Research Institute, using an incident X-ray with the wavelength, $\lambda = 1$ Å. Scattered X-rays were detected using an imaging plate with a resolution of 0.1 mm/pixel and 4 m sample-to-detector distance.

RESULTS AND DISCUSSION

The PBDT solutions before the dialysis are optically isotropic, when $C_P < C_{LC}$*. However, after diffusion of Ca^{2+} for 1 day, they form gel, and the gel shows a strong and uniform birefringence at the two outer regions of the cell (denoted as region I), close to the Ca^{2+} solution, while a weak birefringence appears in the narrow central region (denoted as region II), as observed under polarizing optical microscope (POM); between region I and II,

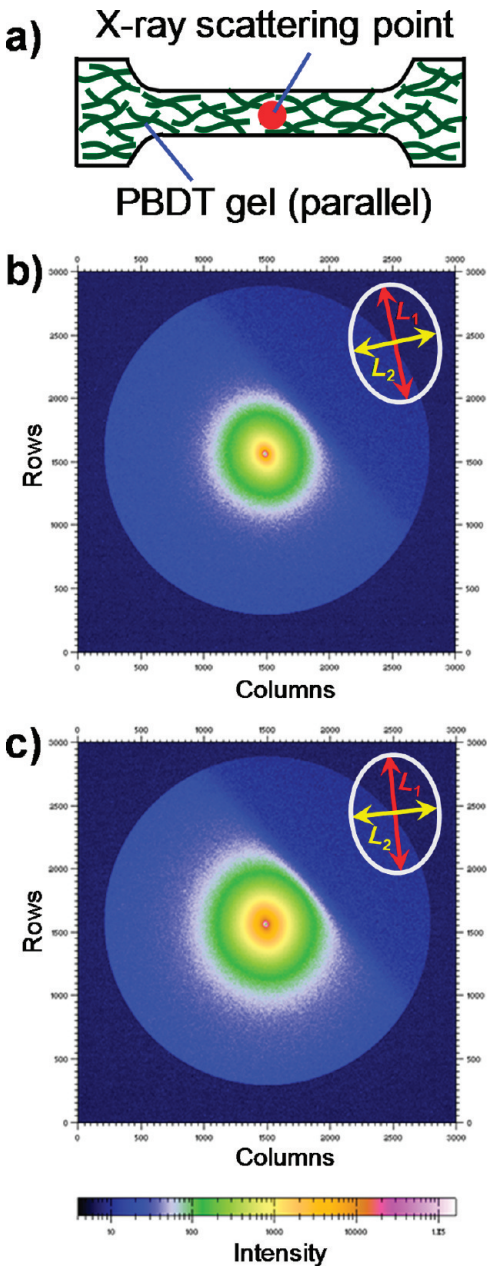

Figure 2. SAXS measurement of the gels. (a) Scheme for scattering position on the specimen. The axis of the dumbbell shape is perpendicular to the ion diffusion direction, as shown in Figure 1c. (b, c) Scattering pattern of the gels synthesized with C_P of 1 wt % (b) and 3 wt % (c). The up-right corner of the scattering pattern is absent due to the placement of imaging plate for wide-angle X-ray scattering. The inset is the schematic of ellipse with the major axis L_1 and minor axis L_2. The weak meridional anisotropic scattering patterns indicate the preferential molecular alignment parallel to the axis of the dumbbell shape specimen, as shown in part a.

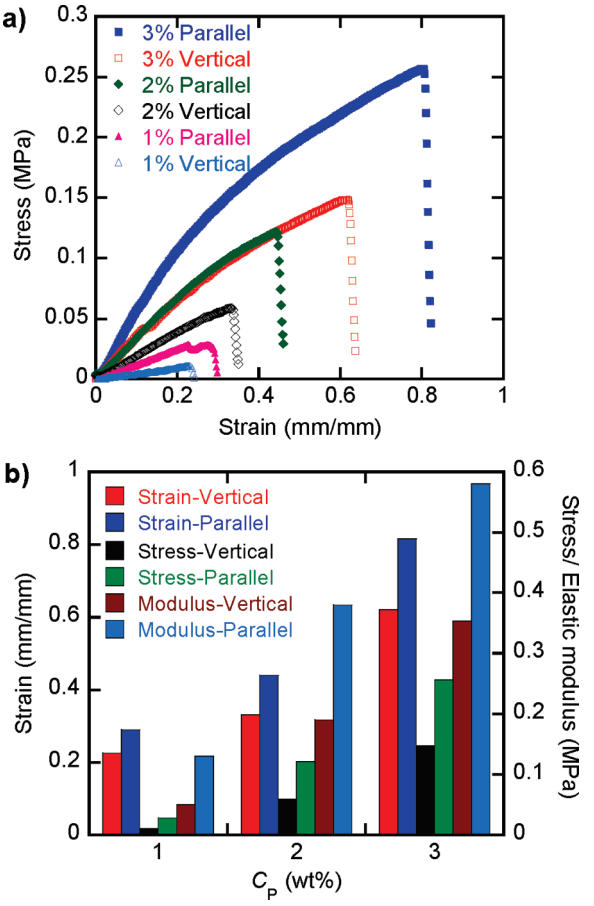

Figure 3. Stress−strain curve (a) and the elastic modulus, fracture strain/stress (b) of physical LC gel (C_P = 1−3 wt %) by elongation parallel and vertical to the PBDT alignment direction. Samples were cut from the outer region of the entire LC gel, as shown in Figure 1c.

amorphous lineal regions are observed (Figure 1b). With insertion of 530 nm tint plate, we found that the region I and region II show different birefringent colors, indicating the different orientations of PBDT molecules in the two regions (Figure 1c). Similar results are observed for high PBDT concentrations (data not shown). To establish the relationship between the PBDT orientation and birefringent color, we observed the birefringence of a PBDT aqueous solution under translational shearing. We found that PBDT has a positive birefringence that shows blue and orange colors when oriented in southwest and northwest directions, respectively, observed with tint plate (Supporting Information, Figure S1).[6e,f,10] Therefore, the birefringent image of Figure 1c indicates that PBDTs orient perpendicular to the diffusion direction in region I, whereas they align parallel to the diffusion direction in region II.

The orientation of PBDT in the region I of the gel is further confirmed by SAXS measurement and tensile test. SAXS and tensile samples are cut from region I of LC gel, as shown in Figure 1c. Figure 2 shows the SAXS results for the samples synthesized with C_P of 1 wt % (b) and 3 wt % (c) and the samples were cut in parallel to the Ca^{2+} diffusion front (in perpendicular to the Ca^{2+} diffusion direction). The elliptical scattering pattern in Figure 2 has a long axis of the ellipsoid in the meridian (ratio of major axis to minor axis, L_1/L_2, is 1.18 ± 0.06 and 1.15 ± 0.03 for Figure 2b and Figure 2c, respectively), indicating that the average distance between PBDT molecules aligned perpendicular to the diffusion direction of Ca^{2+} is slightly shorter than that aligned parallel to the ion diffusion direction. The scattering peak, despite of its weakness, corresponds to a characteristic spacing of 15−20 nm, indicating the long-range spatial correlation among PBDTs, probably due to the strong electrostatic interaction. Surprisingly, such a weak molecular alignment can generate the strong birefringence that should be related to the formation of giant assemblies, the mesoscopic

dx.doi.org/10.1021/ma2001228 |*Macromolecules* 2011, 44, 3535–3541

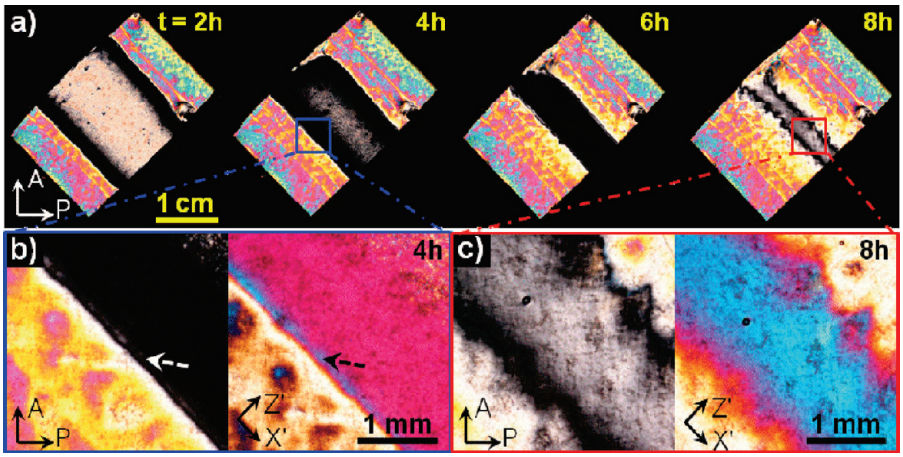

Figure 4. (a) Images of 2 wt % LC gel at different dialysis time observed under polarizing microscope. (b, c) Enlarge images of the diffusion front (b) and the central part of the gel (c); the right micrographs are observed with tint plate. Arrows in part b show the birefringence reversion at the diffusion flux front. The different birefringence colors of region I in part a observed under POM without tint plate are due to the different birefringence that is strong and shifts into the second-order color, rather than the birefringence reversion.

fibrous bundles (will be illustrated in the following), of the semirigid polyanion with the aid of Ca^{2+} diffusion and complexation.

Furthermore, the samples possess relatively higher elastic modulus, *E*, and tensile fracture stress/strain along the direction in parallel to the diffusion front (perpendicular to the diffusion direction) than that perpendicular to the diffusion front, for 1, 2, and 3 wt % PBDT concentration investigated (Figure 3). The elastic modulus, the fracture stress/strain increased with the increase of the PBDT concentration. At the 3 wt % PBDT concentration, the fracture stress and strain reached 0.26 MPa and 81%, respectively, which is relatively strong.

Although these physical PBDT gels are still brittle in comparison with recently developed various kinds of chemically cross-linked hydrogels,[11] the mechanical properties can be substantially improved by using a double-network technique that will be separately described in a following paper.

Both the SAXS results and the tensile test results coincide well with the POM observation in Figure 1c, confirming that PBDT molecules oriented in parallel to the Ca^{2+} diffusion front, that is, PBDTs align perpendicular to the Ca^{2+} diffusion direction. This is different from the results reported for DNA and Curdlan biomacromolecules by Dobashi et al.,[8] in which these biomacromolecules were assigned to orient in parallel to the ion diffusion direction. These results explain why we got a controversial conclusion in our previous work, in which the PBDT orientation was assigned incorrectly.[5d]

To track the diffusion-gelation process, we perform *in situ* observation of the entire gelation process under POM at different dialysis time, as shown in Figure 4a. The original solution with $C_P = 2$ wt % $= C_{LC}^*$ shows a schlieren texture that is characteristic of nematic phase.[10] After 2 h dialysis, the regions neighboring to the Ca^{2+} diffusion front are gelated with slight turbidity, whereas the central part is still in solution. The gel front line moves toward the center of the cell; the width of the gel region (corresponding to region I in Figure 1b) gradually increases with time until the entire sample becomes physical gel. The width of the central solution region (corresponding to region II in Figure 1b) decreases with time, meanwhile the birefringence of the solution gradually vanishes, indicating the decrease in C_P. An interesting phenomenon is that, at the front of the diffusion flux, a very thin ($\sim$100 μm) birefringent layer, shown by the arrow in Figure 4b, exists that accompanies with the progression of the flux toward the center. In this thin layer, PBDT molecules orient parallel to the diffusion direction, as observed with tint plate (Figure 4b). This result indicates that PBDT alignment reverses its direction at the flux front, from the direction parallel to the diffusion direction of Ca^{2+} in the solution region to that perpendicular to the diffusion direction of Ca^{2+} in the gelated region. Finally, the two gelated regions progressed from the two ends of the reaction cell meet in the central region and the flux fronts are terminated. At 8 h, the central region with the width of $\sim$1 mm is also gelated to generate birefringence, with the PBDT oriented in parallel to the diffusion direction of Ca^{2+} (Figure 4c). The final width of the central region after gelation, *W*, increases with the increment of C_P from $W = 0.5$ mm at $C_P = 1$ wt % to $W = 1.5$ mm at $C_P = 2$ wt %.

As shown in Figure 4b, the boundaries between region I and II are sharp and smooth at the initial dialysis state, indicating an abrupt change in the Ca^{2+} concentration at the Ca^{2+} diffusion front that is associated with the cooperative complexation of semirigid PBDTs. However, the boundaries become rough (Figure 4c) in the final dialysis state, probably due to the fluctuation of the Ca^{2+} diffusion front.

To investigate the kinetics of diffusion and gelation, the width of region I of the synthesized plate gels, *d*, is plot versus square root of dialysis time, $t^{1/2}$; it shows a good linear relationship, indicating that the gelation is controlled by the diffusion process (Figure 5). Through the slope of $d/t^{1/2} \sim 0.007$ and Einstein—Stock equation of $d^2 = 2Dt$,[12] we can calculate the apparent diffusion coefficient $D \sim 2.4 \times 10^{-5}$ cm$^2 \cdot$s^{-1} that is quite similar to 1.9×10^{-5} cm$^2 \cdot$s^{-1} observed by Dobashi in the Ca^{2+}—Curdlan system.[8a] This diffusion coefficient is 3—4 times larger than the true diffusion coefficient of Ca^{2+} in pure water, 7.9×10^{-6} cm$^2 \cdot$s^{-1},[13] indicating that the immobilizing of the Ca^{2+} by gelation decreases the local concentration of free Ca^{2+}, and thus promotes the diffusion process.

The central region II of the LC gel has a larger swelling ratio than that of the outer region I (Figure 6), indicating that the some PBDT molecules have diffused from the central region to the outer region (the flux front) for complexation to form LC gel. This result is consistent with the fact that the birefringence

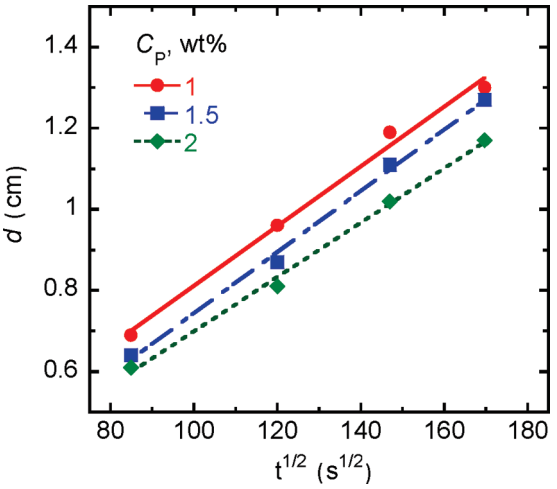

Figure 5. Relationship of the length of LC gel with different C_P values versus dialysis time.

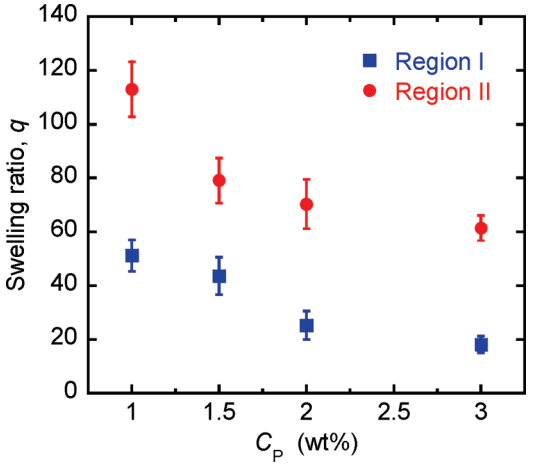

Figure 6. Swelling ratio of the center and outer regions of the gel synthesized with different C_P.

decays and finally vanishes with the progress of the dialysis at the central region, as observed in Figure 4a.

We note that the complexation induces PBDT orientation and formation of mesoscopic fibrous bundles (Figure 7). The multivalent ions bridge like-charged rigid or semirigid polyelectrolytes to form bundles,[14] companying with the release of monovalent counterions.[15] At the diffusion front of Ca^{2+} ions, PBDTs meet with Ca^{2+} and self-assemble to form fibrous bundles. When the Ca^{2+} concentration gradient is high at the diffusion front, it is more energetically favorable for the highly charged PBDT molecules to orient in parallel to the diffusion front, which ensures more complexation. The similar result was reported by Stupp and co-workers, in which aqueous solutions of peptide amphiphile with positive charges were dropped into polyanion solution; the partial charge screening of the peptide amphiphiles led them self-assemble into fibrous bundles aligned parallel to the liquid−liquid interface.[16]

The fibrous bundles of PBDT cannot be directly observed by POM in other gels with $C_P \leq C_{LC}^*$; however, we postulate that the formation of mesoscopic PBDT bundles is universal during

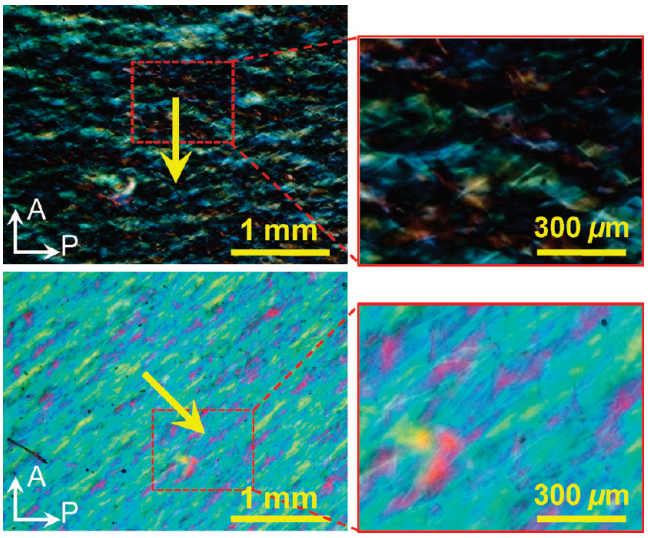

Figure 7. Micrographs of the fibrous structure in the outer region I of 3 wt % PBDT gel observed under polarizing microscope. Arrows show the Ca^{2+} diffusion direction.

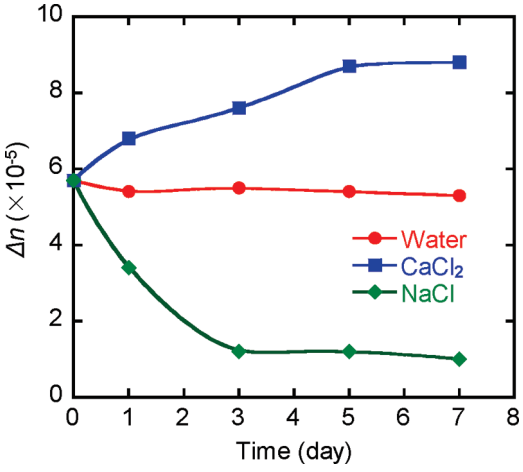

Figure 8. Birefringence change of 1 wt % LC gel with time after reimmersing into pure water, 0.5 M $CaCl_2$ or 1.5 M NaCl aqueous solution.

the complexation and self-assembly process.[9b,14,16] Even the addition of a certain amount of monovalent salt can induce the PBDT molecules self-assembly into submicrometer size bundles.[6b,9b] In the diffusion of Ca^{2+}, high C_P ($C_P > C_{LC}^*$) should favors formation of thick and long fibrous bundles that can just be observable under microscope. It should be noted, as shown by the SAXS results in Figure 2, that the orientation of PBDT bundles is very weak; the staggered fibers in region I of LC gel only have slight directional preference perpendicular to the diffusion direction (Figure 7).

This ordered structure frozen by physically cross-linking is not stable if the gel is immersed in the simple salt solution with strong ionic strength. Figure 8 shows that the birefringence in region I of LC gel decreases with time when immersed in 1.5 M NaCl solution. A high concentration of NaCl may destroy the Ca^{2+} bridging (cross-linking of PBDT) due to the increase in the ionic strength. This can be understood from the dynamic viewpoint:

dx.doi.org/10.1021/ma2001228 |*Macromolecules* 2011, 44, 3535–3541

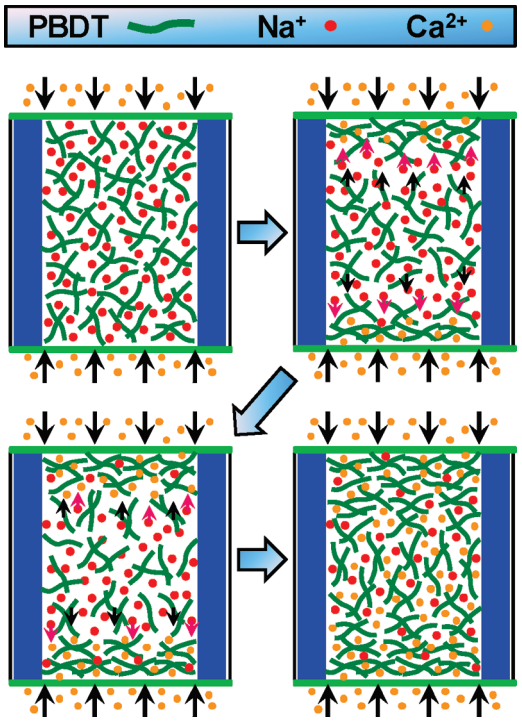

Figure 9. Illustration for anisotropic LC gel formation via dialysis of PBDT solution in Ca^{2+} solution, driven by complexation. Before the Ca^{2+} diffusion, the PBDT solution is macroscopically isotropic even when $C_P > C_{LC}^*$. When the Ca^{2+} diffuses readily into the anionic PBDT solution, the electrostatic complexation and gelation occur at the diffusion front and PBDT molecules simultaneously self-assemble into fibrous bundles. Owing to the large concentration gradient of Ca^{2+}, the semirigid PBDTs orient parallel to the diffusion front (perpendicular to the diffusion direction) to form more stable bundles. Meanwhile, the PBDT molecules in the central region diffuse to the Ca^{2+} flux front due to the local mobile PBDT concentration gradient built. The transversal diffusion (motion) of semirigid PBDT is severely suppressed by the surrounding rod molecules due to steric constraints, while the longitudinal diffusion is barely influenced. As a result, PBDTs at the Ca^{2+} diffusion front show a favorable orientation in parallel to the Ca^{2+} diffusion direction. Finally, the two Ca^{2+} fluxes from the two ends meet, forming the LC gel in the narrow central region with PBDT parallel to the Ca^{2+} diffusion direction. Illustration of PBDT bundles are not shown here for simplicity.

the bonding of Ca^{2+} to PBDT has a finite lifetime, and the exchange of Ca^{2+} always occurs.[17] If the Ca^{2+} concentration is high and there is no or low concentration of monovalent ions, the cross-linking by Ca^{2+} always exists by exchanging with other Ca^{2+} ions. However, if the concentration of Na^+ is high, some of the binding site will be exchanged by Na^+, which destroy the cross-linking structure.[18] On the other hand, the LC gel is stable in pure water. The release of Ca^{2+} in pure water should not occur since there are no other positive ions to substitute for the Ca^{2+}. That is why in water, the structure is relatively stable. If the LC gel is immersed in 0.5 M $CaCl_2$ solution, the birefringence increase from 5.7×10^{-5} to 8.8×10^{-5}, indicating that the PBDTs are further cross-linked by the additional Ca^{2+}. The additional cross-linking process is relatively slow comparing with the gelation during the dialysis, taking 5 days to reach the saturated state. We consider that PBDT−Ca^{2+} complexation is not stoichiometric during the dialysis process because of the limited dialysis time and the existence of monovalent ions.

On the basis of these results, we proposed a possible self-assembly mechanism for PBDT/Ca^{2+} anisotropic gel (Figure 9). Before the Ca^{2+} diffusion, the PBDT solution is *macroscopically* isotropic regardless of the fact that C_P is lower or higher than the critical LC concentration C_{LC}^*. After immersing the reaction cell into $CaCl_2$ solution, the small Ca^{2+} diffuses readily into the anionic PBDT solution through the two semipermeable membranes, leading to the electrostatic complexation along the diffusion front of Ca^{2+} and the simultaneous self-assembly of PBDT molecules into mesoscopic fibrous bundles at the diffusion front.[16] Owing to the sharp concentration gradient of Ca^{2+}, the semirigid PBDTs orient parallel to the diffusion front (perpendicular to the diffusion direction) to form more stable bundles. Meanwhile, the PBDT molecules in the central region diffuse to the Ca^{2+} flux front due to the local PBDT concentration gradient built. During the transportation of PBDT molecules from the central region of solution to the diffusion flux front, the transversal diffusion (motion) of semirigid PBDT is severely suppressed by the surrounding rod molecules due to steric constraints; however, the longitudinal diffusion is barely influenced.[19] As a result, PBDTs at the diffusion flux front show a favorable orientation in parallel to the diffusion direction of Ca^{2+}. Finally, the two Ca^{2+} fluxes from the two ends meet, forming the LC gel in the narrow central region with PBDT alignment parallel to the diffusion direction of Ca^{2+}.

The structure of PBDT LC gel is quite different from the DNA or Curdlan gel by Dobashi et al., of which biomacromolecules were reported align parallel to the diffusion direction of multivalent cations, forming a radial physical gel in dialysis tube.[8] The differences might stem from two reasons. First, PBDT and the biomacromolecules have different molecular rigidity, charge density and cooperative coupling with multivalent cations that should lead to different self-assembly behaviors and molecular orientation. Second, in Dobashi's work, the biomacromolecules were dissolved in buffers such as sodium hydroxide for Curdlan or mixture of sodium borate and sodium chloride for DNA. The existence of simple salts screens the electrostatic interaction between these charged macromolecules and the multivalent ions, so the complexation is less vigorous in the presence of simple salt. Additionally, we failed to find clear evidence in the literatures to show that these biomacromolecules align parallel to the diffusion direction of multivalent cations. So there remains a possibility that in these systems, the biomacromolecules also orient in perpendicular to the diffusion direction.

■ CONCLUSIONS

We have developed macroscopically anisotropic hydrogels by dialysis of a synthetic semirigid polyanion poly(2,2′-disulfonyl-4,4′-benzidine terephthalamide) (PBDT) in aqueous solution of Ca^{2+}. The PBDT molecular orientation and physical gelation are induced and controlled by the Ca^{2+} diffusion process. The electrostatic complexation between the cationic Ca^{2+} and anionic PBDT results in the self-assembly of PBDT molecules into mesoscopic fibrous bundles that align in parallel to the Ca^{2+} flux front (i.e., perpendicular to the diffusion direction of Ca^{2+}). At the local flux front, PBDT molecules diffuse from the solution phase due to the concentration gradient, resulting in the PBDT alignment parallel to the diffusion direction of Ca^{2+} to form a thin anisotropic layer due to the favorable longitudinal diffusion during PBDT transportation. Finally, the different oriented structures of PBDT are frozen to form LC gels, of which PBDT

dx.doi.org/10.1021/ma2001228 |*Macromolecules* 2011, 44, 3535–3541

aligns perpendicular to the diffusion direction of Ca^{2+} in the outer regions and parallel to the diffusion in the narrow central region. The extraordinary molecular reorientation at the diffusion flux front and complex molecular alignments in the physical hydrogel are observed for the first time and expected to merit revealing the formation of oriented structures in living organisms and find applications in materials sciences, such as optical sensors.

■ ASSOCIATED CONTENT

Supporting Information. Micrographs showing shear-induced birefringence of PBDT solution. This material is available free of charge via the Internet at http://pubs.acs.org.

■ AUTHOR INFORMATION

Corresponding Author

*E-mail: gong@mail.sci.hokudai.ac.jp.

Present Addresses

#Yamagata University, 4-3-16 Jonan, Yonezawa-shi, Yamagata 992−8510, Japan.

■ ACKNOWLEDGMENT

This research was financially supported by a Grant-in-Aid for Specially Promoted Research (No. 18002002) from the Ministry of Education, Science, Sports, and Culture of Japan. The authors thank Dr. Yasuyuki Maki for the helpful discussion.

■ REFERENCES

(1) (a) Fung, Y. C. *Biomechanics: Mechanical properties of living tissues*, 2nd ed.; Springer-Verlag Inc.: New York, 1993. (b) Gartner, L. P.; Hiatt, J. L. *Color Textbook of Histology*, 2nd ed.; Saunders: Philadelphia, PA, 2001.

(2) (a) Sanchez, C.; Arribart, H.; Giraud-Guille, M. M. *Nat. Mater.* **2005**, *4*, 277. (b) Coppin, C. M.; Leavis, P. C. *Biophys. J.* **1992**, *63*, 794.

(3) (a) Branden, C.; Tooze, J. *Introduction to Protein Structure*, 2nd ed.; Taylor & Francis: New York, 1999. (b) Tang, J. X.; Janmey, P. A. *J. Biol. Chem.* **1996**, *271*, 8556. (c) Liu, X. D.; Diao, H. Y.; Nishi, N. *Chem. Soc. Rev.* **2008**, *37*, 2745.

(4) (a) Hartgerink, J. D.; Beniash, E.; Stupp, S. I. *Science* **2001**, *294*, 1684. (b) Perumal, S.; Antipova, O.; Orgel, J. P. *Proc. Natl. Acad. Sci. U.S.A.* **2008**, *105*, 2824. (c) Hirst, L. S.; Pynn, R.; Bruinsma, R. F.; Safinya, C. R. *J. Chem. Phys.* **2005**, *123*, 104902. (d) Conwell, C. C.; Hud, N. V. *Biochemistry* **2004**, *43*, 5380. (e) Zhu, N.; Liggitt, D.; Liu, Y.; Debs, R. *Science* **1993**, *261*, 209. (f) Kwon, H. J.; Kakugo, A.; Ura, T.; Okajima, T.; Tanaka, Y.; Furukawa, H.; Osada, Y.; Gong, J. P. *Langmuir* **2007**, *23*, 6257.

(5) (a) Kato, T.; Mizoshita, N.; Kishimoto, K. *Angew. Chem., Int. Ed.* **2006**, *45*, 38. (b) Clapper, J. D.; Guymon, C. A. *Adv. Mater.* **2006**, *18*, 1575. (c) Um, S. H.; Lee, J. B.; Park, N.; Kwon, S. Y.; Umbach, C. C.; Luo, D. *Nat. Mater.* **2006**, *5*, 797. (d) Yang, W.; Furukawa, H.; Gong, J. P. *Adv. Mater.* **2008**, *20*, 4499. (e) Chung, H. J.; Park, T. G. *Nano Today* **2009**, *4*, 429. (f) Every, H. A.; Van der Ham, L. V.; Picken, S. J.; Mendes, E. *Soft Matter* **2009**, *5*, 342. (g) Gao, Y.; Zhao, F.; Wang, Q.; Zhang, Y.; Xu, B. *Chem. Soc. Rev.* **2010**, *39*, 3425.

(6) (a) Shigekura, Y.; Chen, Y. M.; Furukawa, H.; Kaneko, T.; Kaneko, D.; Osada, Y.; Gong, J. P. *Adv. Mater.* **2005**, *17*, 2695. (b) Shigekura, Y.; Furukawa, H.; Yang, W.; Chen, Y. M.; Kaneko, D.; Osada, Y.; Gong, J. P. *Macromolecules* **2007**, *40*, 2477. (c) Wu, Z. L.; Furukawa, H.; Yang, W.; Gong, J. P. *Adv. Mater.* **2009**, *21*, 4696. (d) Wu, Z. L.; Kurokawa, T.; Liang, S. M.; Gong, J. P. *Macromolecules* **2010**, *43*, 8082. (e) Wu, Z. L.; Kurokawa, T.; Liang, S. M.; Furukawa, H.; Gong, J. P. *J. Am. Chem. Soc.* **2010**, *132*, 10064. (f) Wu, Z. L.; Arifuzzaman, M.; Kurokawa, T.; Furukawa, H.; Gong, J. P. *Soft Matter* **2011**, *7*, 1884.

(7) (a) Henisch, H. K. *Crystals in Gels and Liesegang Rings*: Cambridge University Press: Cambridge, U.K., 1988. (b) Grzybowski, B. A.; Bishop, K. J. M.; Campbell, C. J.; Fialkowski, M.; Smoukov, S. K. *Soft Matter* **2005**, *1*, 114.

(8) (a) Dobashi, T.; Nobe, M.; Yoshihara, H.; Konno, A. *Langmuir* **2004**, *20*, 6530. (b) Nobe, M.; Dobashi, T.; Yamamoto, T. *Langmuir* **2005**, *21*, 8155. (c) Dobashi, T.; Furusawa, K.; Kita, E.; Minamisawa, Y.; Yamamoto, T. *Langmuir* **2007**, *23*, 1303. (d) Furusawa, K.; Minamisawa, Y.; Dobashi, T.; Yamamoto, T. *J. Phys. Chem. B* **2007**, *111*, 14423. (e) Furusawa, K.; Narazaki, Y.; Tomita, N.; Dobashi, T.; Sasaki, N.; Yamamoto, T. *J. Phys. Chem. B* **2010**, *114*, 13923.

(9) (a) Vandenberg, E. J.; Diveley, W. R.; Filar, L. J.; Pater, S. R.; Barth, H. G. *J. Polym. Sci, Part A: Polym. Chem.* **1989**, *27*, 3745. (b) Yang, W.; Furukawa, H.; Shigekura, Y.; Shikinaka, K.; Osada, Y.; Gong, J. P. *Macromolecules* **2008**, *41*, 1791.

(10) Demus, D.; Goodby, J.; Gray, G. W.; Spiess, H. W.; Vill, V. *Handbook of Liquid Crystals*: Wiley-VCH: Weinheim, Germany, 1998.

(11) (a) Okumura, Y.; Ito, K. *Adv. Mater.* **2001**, *13*, 485. (b) Haraguchi, K.; Takehisa, T. *Adv. Mater.* **2002**, *14*, 1120. (c) Gong, J. P.; Katsuyama, Y.; Kurokawa, T.; Osada, Y. *Adv. Mater.* **2003**, *15*, 1155. (d) Tanaka, Y.; Gong, J. P.; Osada, Y. *Prog. Polym. Sci.* **2005**, *30*, 1.

(12) Einstein, A. *Investigations on the theory of Bromnian movement*, Dover: New York, 1926.

(13) Lide, D. R. *Handbook of Chemistry and Physics*, 76th ed.; CRC Press: Boca Raton, FL, 1995.

(14) Butler, J. C.; Angelini, T.; Tang, J. X.; Wong, G. C. L. *Phys. Rev. Lett.* **2003**, *91*, 028301.

(15) (a) Wagner, K.; Harries, D.; May, S.; Kahl, V.; Rädler, J. O.; Ben-Shaul, A. *Langmuir* **2000**, *16*, 303. (b) Gummel, J.; Cousin, F.; Boué, F. *J. Am. Chem. Soc.* **2007**, *129*, 5806.

(16) (a) Capito, R. M.; Azevedo, H. S.; Velichko, Y.; Mata, S. A.; Stupp, S. I. *Science* **2008**, *319*, 1812. (b) Carvajal, D.; Bitton, R.; Mantei, J. R.; Velichko, Y. S.; Stupp, S. I.; Shull, K. R. *Soft Matter* **2010**, *6*, 1816.

(17) (a) Narita, T.; Gong, J. P.; Osada, Y. *J. Phys. Chem. B* **1998**, *102*, 4566. (b) Narita, T.; Hirota, N.; Gong, J. P.; Osada, Y. *J. Phys. Chem. B* **1999**, *103*, 6262.

(18) Baumberger, T.; Ronsin, O. *Biomacromolecules* **2010**, *11*, 1571.

(19) (a) Szamel, G. *Phys. Rev. Lett.* **1993**, *70*, 3744. (b) Cush, R.; Dorman, D.; Russo, P. S. *Macromolecules* **2004**, *37*, 9577. (c) Munk, T.; Höfling, F.; Frey, E.; Franosch, T. *Europhys. Lett.* **2009**, *85*, 30003.